Perovskite Solar Cells Instability Under Reverse Bias

R. A. Z. Razera,[1,2] D. Jacobs,[1] P. Fiala,[1] M. Dussouillez,[3] F. Sahli,[1] F. Fu,[1] T. C. Yang,[1] L. Ding,[3] A. Walter,[3] S. Nicolay,[3] A. F. Feil,[4] H. Boudinov,[2] Q. Jeangros,[1] and C. Ballif[1,3]

[1)] *École Polytechnique Fédéral de Lausanne (EPFL), Institute of Microengineering (IMT) Photovoltaics and Thin-Film Electronics Laboratory (PV-Lab), Rue de la Maladière 71b, Neuchâtel 2002, Switzerland*

[2)] *Universidade Federal do Rio Grande do Sul (UFRGS), Laboratório de Microeletrônica, Av. Bento Gonçalves 9500, Porto Alegre-RS, Brazil*

[3)] *CSEM, PV-Center, Jaquet-Droz 1, 2002 Neuchâtel, Switzerland*

[4)] *Pontifícia Universidade Católica do Rio Grande do Sul (PUCRS), Escola de Ciências, Av. Ipiranga, 90619-900, 6681, Porto Alegre-RS, Brazil*

(Dated: 1 August 2019)

Partial shading of a photovoltaic module may trigger the permanent damage of the shaded cells as the latter are driven into reverse bias by the illuminated cells. Perovskite solar cells have been shown to degrade quickly when experiencing such field-relevant conditions due to processes that have remained elusive. Here, we combine several imaging and optoelectronic characterization techniques to elucidate the mechanisms governing degradation in reverse bias. Three main processes are shown to occur in cesium formamidinium lead iodide bromide cells depending on biasing conditions. The most severe involves the formation of shunts at the position of the metal electrode. Second, iodide is driven into the electron transport layer, which causes an S-shape in the current-voltage curve. And third, the perovskite absorber is shown to segregate into iodide- and bromide-rich domains, shifting the overall band gap and changing the perovskite microstructure. While the S-shape formation process is reversible, the other two mechanisms affect irreversibly the optoelectronic properties of the cell. Finally, the criteria that must be met to pass partial shading tests defined by the International Electrotechnical Commission are discussed.

Keywords: perovskite solar cells, reverse bias, instability, shunting, S-shape, phase segregation

I. INTRODUCTION

Photovoltaic modules may become partially shaded during operation as a result of various factors such as a nearby building or tree, sand, snow, bird droppings or even when cleaned during sunlight exposure. In these conditions, the shaded cells cannot produce as much current as the illuminated ones and the latter will drive the shaded cells into reverse bias. Depending on the fraction of the module that is shaded, the breakdown voltage of the shaded cells and the possible presence of shunts (defined here as direct contacts between top and bottom electrodes), all the current produced by the illuminated cells can flow through a small area of the shaded cell(s). The large current densities that result may cause excessive heating, damaging the cell and/or the encapsulant[1]. As a testament to the severity of the damage that may be induced by these partial shading conditions, the International Electrotechnical Co mission (IEC) has set up a reliability protocol to test modules[2]. The test consists in two parts. In the first one, the cell with the highest leakage current is identified. The second part involves fully and then partially shading the identified cell of the module under a sun simulator to maximize the power dissipated in the shaded cell. The test does not provide any pass/fail requirement for the power loss, except that no major visual damage should appear in the cells or the module encapsulant during the test.

Although the use of bypass diode can limit the reverse voltage applied on shaded cells[1,3,4], these add cost to the module. It is hence desirable to make the solar cells as resilient against reverse voltage as possible and to minimize the number of bypass diodes. In the worst case scenario (economically), one bypass diode per cell is needed and the reverse voltage on the solar cell is limited to the turn-on voltage of the bypass diode, which can be as low as ~ 0.3 V[3]. In the best case, the breakdown voltage of the cell is sufficiently low so that the shaded cell itself sinks all the current of the illuminated part of the segment. In this ideal situation, the reverse voltage applied to the shunts (equal to the breakdown voltage of the shaded cell, V_{bd}, since the shunts are in parallel to the active area) remains low, meaning that no hot spots are created and no bypass diodes are needed. This assumes the active area of the cell can endure a reverse bias equal to V_{bd}, a reverse current equal the current at maximum power point I_{mpp} and hence a power dissipation of $V_{bd} \times I_{mpp}$ without degrading. It also assumes V_{bd} can be engineered in the first place.

While the effects of partial shading and hot spot formation in crystalline silicon (c-Si) modules are now well investigated[1,3–6], this is not case for the nascent perovskite solar cell technology. A first detailed study was reported only recently by Bowring et al[7]. The authors demonstrated that perovskite cells degraded quickly in such conditions as hot spots appeared under the metal electrode in just a few minutes at low reverse voltages (¿-1 V). Even in the absence of hot spots, the cell series resistance was found to increase, while the V_{oc} lowered, presumably as a result of an electrochemical reaction between the perovskite absorber and the adjacent layers.

However, only indirect evidence was provided and it remains unclear which species were reacting.

Here, we combine several imaging and optoelectronic characterization techniques to directly assess these degradation mechanisms induced by a reverse bias, i.e. shunt formation and interfacial reaction, before highlighting the appearance of third phenomenon: current-induced phase segregation. We conclude by analyzing the engineering requirements to avoid a degradation of perovskite cells in reverse bias.

II. MECHANISMS OF DEGRADATION

A. Shunt Formation

The perovskite composition studied in this work is $(FAPbI_3)_{0.83}(CsPbBr_3)_{0.17}$, with a band gap of 1.64 eV. The cell is depicted in Figure 1a and the fabrication methods are detailed in the supporting information. It should be noted that a semi-transparent structure is studied in this work, where silver is deposited as fingers on top of a transparent conductive oxide. We focus on this structure as it is the one used as a top cell in Si/PK or PK/PK multi-junctions[8].

To assess the degradation of perovskite solar cells, the reverse bias is progressively increased in steps of -0.1 V up until reaching a value of -2 V or higher. The cell is kept for 3 minutes, before acquiring a current-voltage (I-V) curve in forward (-0.1 V to 1.2 V) and in reverse (1.2 V to -0.1 V) to monitor any change in performance. Typical I-V evolution sequences obtained with this procedure are shown in Figure S1. Some hysteresis is observed, but both forward and reverse scans present similar characteristics after reverse biasing (Figure S2). For clarity, only forward scans are shown in the core of this manuscript. While significant cell-to-cell and batch-to-batch variations are observed in terms of absolute I-V properties (short circuit current, I_{sc}, open circuit voltage, V_{oc}, or fill factor FF) as also noted by Bowring et al[7], the trends described below were found to be universal.

A representative evolution of the I-V curve (forward scan) of a cell after it had been reverse biased in steps is shown in Figure 1b. Two degradation mechanisms occur in succession. For voltages less (in absolute value) than -1.2 V, an S-shape appears, while for higher voltages the cell becomes shunted, as observed from the step decrease in V_{oc} and the increase in slope at $V = 0$ V. Figure 1c reports the reverse current that flows through the cell at each reverse bias step. Up until the -1.1 V, the reverse current is negligible (less than 1 $mAcm^{-2}$). After about 2.6 min at -1.2 V, the current suddenly increases more than 50 $mAcm^{-2}$, signaling the formation of shunt(s). In addition, burst noise[9], typically associated to metal precipitates inside semiconductor devices, appears at this point.

To verify that shunts are indeed forming, a fresh device is analyzed by dark lock-in thermography[10]. The device is first driven to forward bias, with the resulting thermograph exhibiting no hot spots (top left panel of Figure 1d). Then, bringing the cell to a reverse bias of -1.5 V in the thermography system induces the formation of two hot spots at the position of the Ag frame (middle panel in Figure 1d). When driving the cell back into forward bias (bottom right thermograph in Figure 1d), the two hot spots remain, indicating that these shunts were formed during the reverse bias treatment and the cell remained shunted when to driven back to a reverse bias.

For cells stressed up to voltages of -5 V instead of -2 V, shunts become severe enough so that burn marks are visible by the naked eye, as shown in Figure S3. In fact, the metal top contact can be seen from the glass side in the regions of the burn marks. This demonstrates the propensity of Ag to penetrate the perovskite and reach the back electrode, creating shunts. And once the shunts are formed, the high power dissipated in these regions degrades quickly the absorber (which becomes porous with Pb-rich inclusions) and the Ag electrode (which clusters in some regions) as highlighted by the scanning electron microscopy images in Figure S3.

Different metals (Cu, Ni, Cr, Al) were also tested as top electrode. But all cell designs were found to be prone to shunting in a similar way to Ag (Figure S4). Regular opaque cells, where Ag is deposited directly on the electron transport layer, here C60, were also tested. Their stability in reverse bias is even worse as shunts appear at reverse voltages of -0.3 V (Figure S5).

The shunting issue observed here for PK cells differs from that occurring in regular c-Si modules. In the case of perovskites, shunts are created by the reverse bias itself. For c-Si cells, the shunts which form hot spots in reverse bias are introduced during cell manufacturing. And in that case, hot spots form in the voltage range where the shunts become the dominant current pathway, i.e. when the breakdown voltage of the diode has not been reached (which can be tens of volts for c-Si cells). Thin film modules (thin-film Si, CIGS or CdTe) are also prone to shunt formation in reverse bias conditions induced by partial shading[11,12].

B. S-shape development

Before shunting, an S-shape is observed to form as the reverse bias increases (Figure 1b). As this S-shape depends on pre-biasing conditions prior to I-V measurements, the effect is expected to be related to mobile ions within the perovskite[13,14]. We hence hypothesize that the cause of this S-shape is the same as the one that induced the increase in series resistance observed by Bowring et al.[7], who suggested that it was linked to an electrochemical reaction between mobile ions and contact layers.

This S-shape formation process was then investigated using scanning transmission electron microscopy (STEM) coupled to energy dispersive X-ray (EDX) spectroscopy.

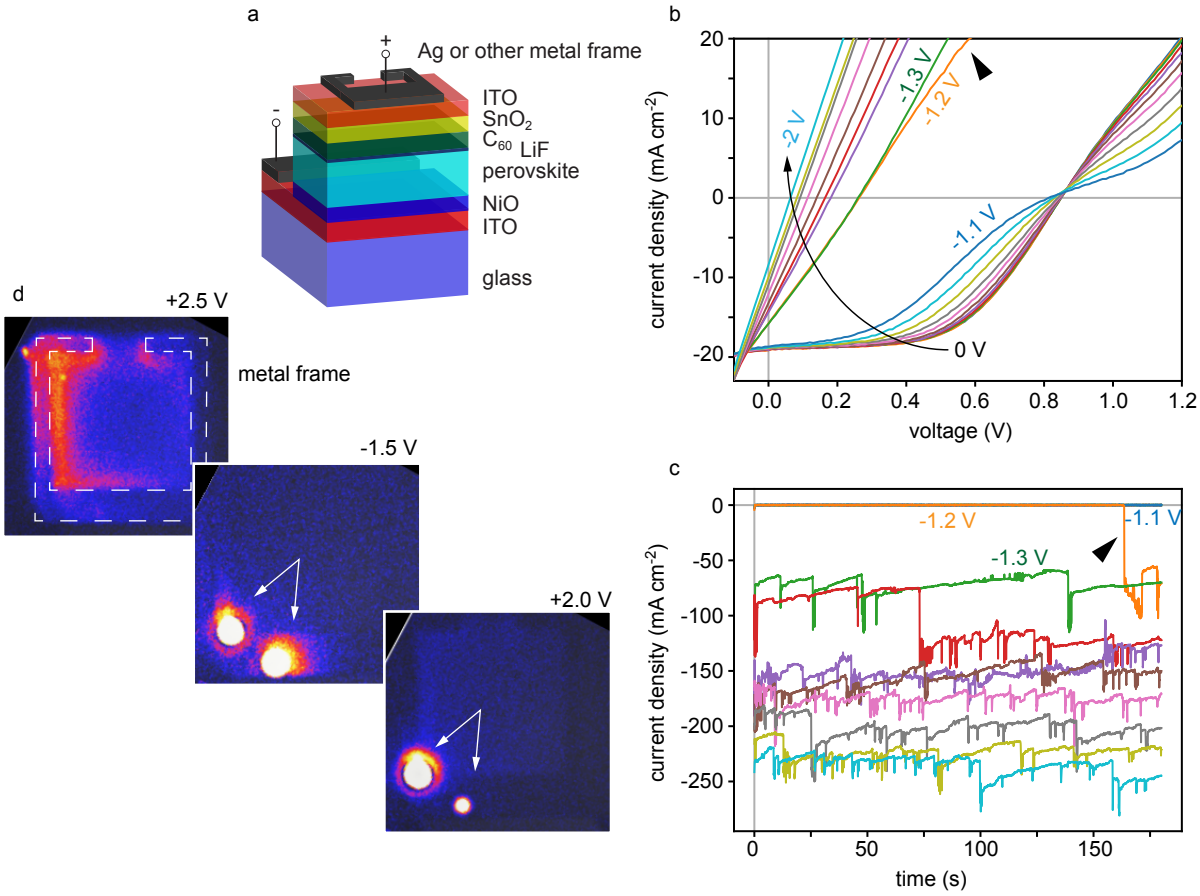

FIG. 1. (a) Structure of the cell studied in this work. The "+" and "-" signs indicate reverse bias. (b) Current-voltage (I-V) curves taken immediately after biasing the cell at progressively higher (in absolute value) reverse voltages. (c) Reverse current measured during the 3 min of each step of reverse biasing. (d) Left: Thermograph of fresh cell, measured with a forward bias of 2.5 V. Middle: same cell at a reverse bias of -1.5 V, showing two new hot spots. Right: same cell under forward bias conditions at 2 V after being reverse biased at -1.5 V, demonstrating that the shunts that formed in the reverse bias step are still present.

Figure 2a shows a STEM high angle annular dark-field image of the cross-section of a cell degraded in reverse bias up to −5 V in a region far from the metal electrode. While the S-shape becomes masked by the shunt in the I-V curve, active regions away from the metal electrode (and hence shunts) should still be affected by the mechanism. Apart from the formation of large voids indicative of a loss of material either during the biasing experiments or during the TEM sample preparation by focused ion beam (FIB), the cell exhibits a double layer microstructure, with the top layer being smoother. For comparison, a STEM image of an as-deposited reference cell is shown in Figure S6. The reference cell also presents voids, although of a smaller size and likely induced by the FIB preparation, but does not show any double layer structure, highlighting that the latter feature is caused by the reverse bias treatment (and not sample preparation). The EDX chemical map and atomic concentration line profile shown in Figure 2b provides more information on this double layer microstructure as the top layer is rich in Br, while the bottom one is richer in I. This evidence of phase segregation is discussed in the next section.

As hinted by Figure 2b, the magnified view of the perovskite/LiF/C_{60} interface shown in Figure 2c demonstrates that I migrated beyond the LiF and into the C_{60} layer. On the other hand, the Cs, Pb and Br EDX signals do not extend as far into the C_{60} (note that some overlap between the different layers is induced by projection effects as the perovskite layer exhibits some roughness and the sample is about 100 nm-thick). Reverse bias-induced halide migration into the electron selective contact was also observed in a previous study employing *in situ* TEM[15]. Doping of C_{60} with halogen has been the subject of several studies[16,17]. These concluded that halogens were incorporated in C_{60} as X_2. As iodine is driven into C_{60} layer by applying a positive bias on the latter, it appears more likely that it is present in its ionized from (I^-). Overall, this EDX data strongly indicates that I^- is driven into the positively biased C_{60} layer. This injection of ions into the electron selective contact may alter the extraction of electrons, as are the changes I and Br distribution in the absorber, and hence induce the

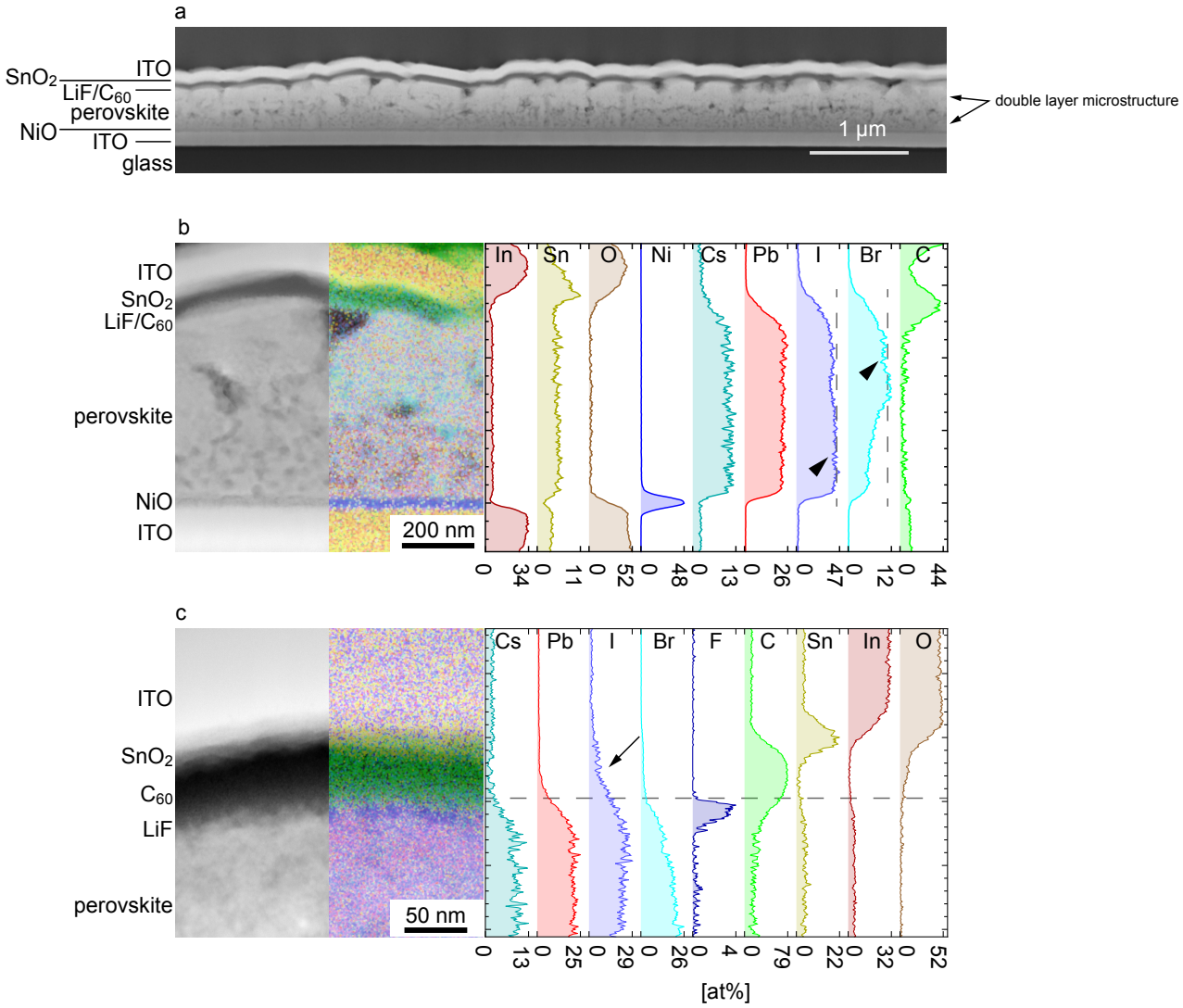

FIG. 2. (a) Scanning transmission electron microscopy (STEM) high angle annular dark-field (HAADF) image of a solar cell degraded at −5 V, showing large voids and a double layer structure. (b) STEM HAADF image of the cell shown in (a) superimposed on its right side with its corresponding EDX chemical map and corresponding concentration profile quantified using the Cliff-Lorimer method. As indicated by arrowheads, the Br concentration increases in the upper part of the absorber, while an inverse trend is noticed for I. The Sn signal inside the PK layer is an artifact caused by the proximity in energy of Sn and I characteristic X-rays. (c) STEM HAADF image and corresponding EDX chemical map and concentration profile of a sample with an higher Br content taken in the region close to the perovskite/LiF/C_{60} interface, which highlights the migration of iodide into the C_{60} layer during reverse biasing (arrowed).

S-shape observed in Figure 1b.

This S-shape formation mechanism appears to be reversible to some extent. To investigate this reversibility, solar cells that do not feature any metal front electrode to avoid any irreversible shunting are reverse biased according to the same procedure described above. As shown in Figure 3a, the absence of metal indeed prevents the formation of shunts. On the other hand, the S-shape gets progressively more severe as the reverse voltage is increased. After degradation, the cell was submitted to maximum power point tracking (MPPT) for about 1 h (Figure 3b), which enabled to recover the initial efficiency (Figure 3c, 7.3%, a low value that results from the high series resistance caused by the lack of metal electrode). While the efficiency are similar before degradation and after MPPT, the I-V curves differ at voltages higher than V_{oc} (Figure 3c). This difference may become smaller with longer MPPT, but it remains unclear to which extent this reaction is reversible. Alternatively, leaving the cell in the dark for 1 hour enables only a partial recovery.

The difference in recovery rate between the dark and MPPT treatments is a first indication that iodide migration into C_{60} is the cause of the S-shape instead of phase segregation. Indeed, applying a negative voltage

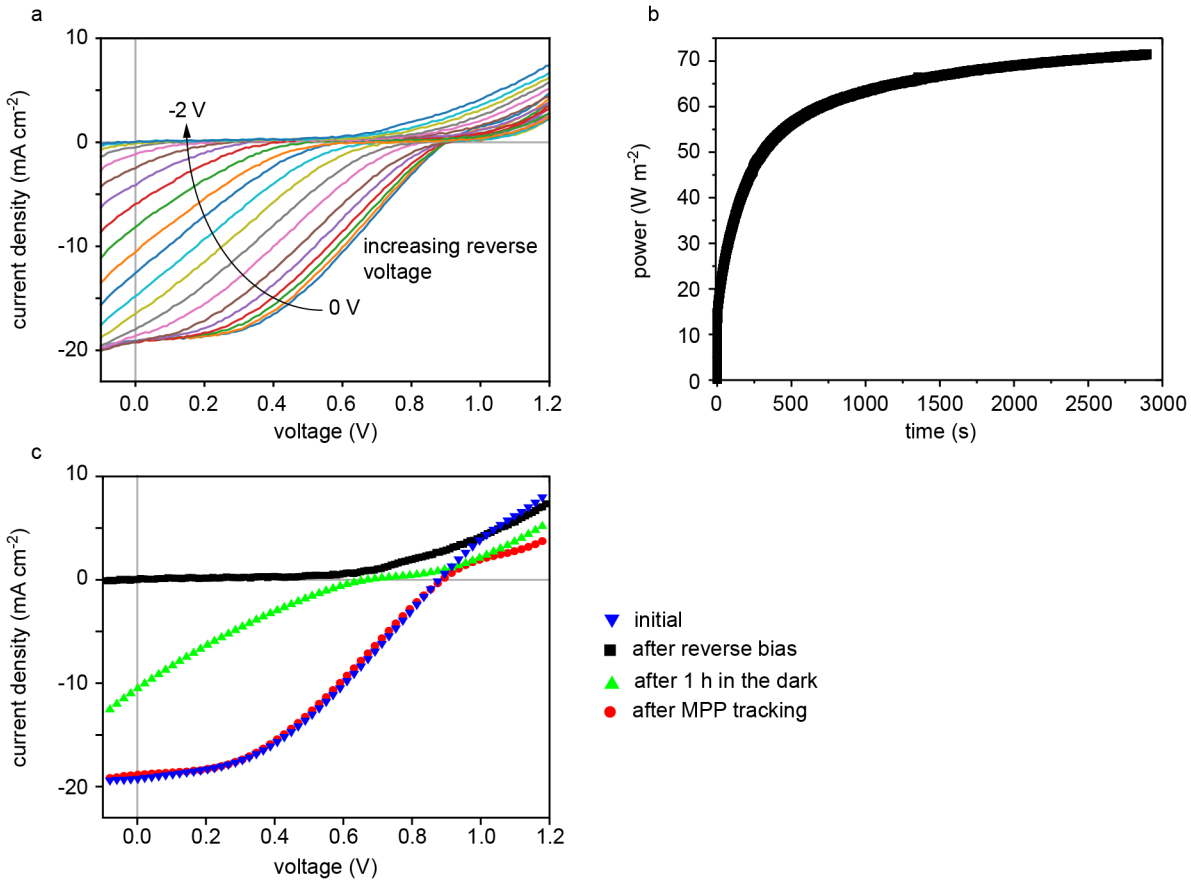

FIG. 3. (a) I-V curves of a cell without any metal electrode taken after progressively increasing the value of the reverse bias. While a severe S-shape builds up, no shunts appear. (b) Maximum power point tracking of the same cell after degradation, showing that the efficiency recovers. (c) Comparison of the I-V curves of the same cell in its fresh state, immediately after reverse biasing, after 1 h in the dark and after maximum power point tracking.

on the C_{60}, as done during MPPT, accelerates the recovery, presumably by pushing I^- back towards the perovskite absorber. Furthermore, ionic motion within the absorber may result in ionic screening of the bulk electric field (which, combined with surface recombination, can cause hysteresis in perovskite solar cells[13,14]) and in turn in S-shapes. But this mechanism can be recovered over timescales of a few seconds/minutes, which is much faster than the recovery rate observed here

Overall, it appears likely that the migration of I^- into the C_{60} may induce non-ohmic series resistance and hence an S-shape at V_{oc}. This non-ohmic resistance may arise from the fact that iodide may act as p-type dopant in C_{60}, decreasing the electron extraction efficiency at the PK/LiF/C_{60} interface. Or from the fact that iodide may decrease the electron mobility in C_{60} so that the non-linear space chargelimited current mechanism starts to become important in the bulk of the C_{60} layer.

C. Phase segregation

Phase segregation of mixed halide perovskites into I-rich (low bandgap) and Br-rich (high bandgap) regions was first reported by Hoke et al.[18]. Since this first study, significant progress has been made to identify the causes and implications of this mechanism[19–25]. Overall, phase segregation was shown to be driven by injection of carriers into the perovskite (by light or current) and by the gradient in strain that results.

Here, a first direct evidence of reverse bias-induced phase segregation was obtained using electron microscopy (Figure 2b). The sample investigated by STEM EDX experienced a reverse bias of -5 V, an absolute value higher than the V_{bd} of the cell (-1 V to -2 V). In turn, a high current passed through the cell (about 1 A cm^{-2}), inducing phase segregation. The steady state photoluminescence (PL) spectra shown in Figure 4a are further indications of the phase segregation induced by this injection of current. There, a fresh device was reverse biased at -3 V for 15 min, before measuring its PL

signal from both sides of the sample (excitation wavelength of 514 nm, absorption depth of about 120 nm). A red-shift of about 0.02 eV in bandgap is observed when measured from the NiO side, agreeing with the I-rich region observed in the TEM image. Alternatively, only a slight blue-shift (approximately 0.005 eV) is measured from the C_{60} side, also in accordance with the EDX data when comparing Figures 2b and S6. It should be noted that the PL laser did not induce any phase segregation on its own as no shift in bandgap is observed with an exposure time of 1 min, a timescale six times longer than the measurement of 10 s.

Duong et al.[19] also observed phase segregation when forward biasing perovskite cells but reported a negligible segregation when a applying a reverse voltage -1 V for 12 h. While the V_{bd} of the cell was not reported, it can be assumed that -1 V did not enable to pass breakdown and negligible current was injected in the absorber. A similar situation was achieved in Figure 4b, which provides the PL data of a sample biased at -0.5 V for 15 min, an absolute value below the V_{bd} of -1 V of this cell. No bandgap shift is observed, in agreement with the need to inject carriers to trigger phase segregation[24].

It should be noted that the shifts observed here depend not only on the extent of the phase segregation (induced by current injection during reverse biasing) but also on the lifetime of the carriers in the device. With long lifetimes, all the carriers generated will migrate to the lower bandgap region and emit a lower energy photon, irrespective of the side that is illuminated. Indeed, the PL spectra acquired from the NiO and C_{60} sides are shifted to the same lower energy when reverse biasing at -5 V for 30 min (Figure S7). irrespective of the side of the sample from which PL was measured. This difference between Figures 4a and S7 is indicative of a difference in carrier lifetime, with carriers being able to reach the lower bandgap region in the latter case.

Figure S8 shows PL spectra acquired from each side of the sample, whose I-V properties are reported in Figure 3a. Even though the I-V curve presented in Figure 3a exhibits a severe S-shape, no shift in bandgap is observed via PL. This observation further confirms first that phase segregation results from current injection when reaching the breakdown voltage threshold and second that phase segregation is not the cause of the S-shape at V_{oc}.

It is worth mentioning that the kinetics of phase segregation can be different between the light- or bias-induced cases[24]. Reverse bias-induced segregation remains visible for days, while its light-induced counterpart usually disappears in a matter of minutes to hours[21,23]. Indeed, the STEM data shown in Figure 2a-b was acquired one week after the sample had been degraded in reverse bias. PL shifts also persisted one week after reverse biasing (Figure S9). This difference in re-homogenization rate between the current- and light-induced cases may stem from the fact that the perovskite absorber segregated by reverse biasing also exhibited severe microstructural changes compared to its as-deposited state (Figure 2-b and Figure S6). These changes in microstructure were presumably induced by the high current that passed through the cell. And these are likely to inhibit any re-homogenization of the elemental distribution.

It should be noted that Bowring et al.[7] did not mention any phase segregation effect in their study on hte reverse bias stability of perovskite cells. However, they reported I-V curves of a sample first degraded in the dark with a current equivalent to $-I_{mpp}$ and then recovered at MPPT for 3h. The I-V curve after recovery had a J_{sc} higher by at least 2 mAcm^{-2} and a V_{oc} lower by about 100 mV compared to before degradation. While the V_{oc} loss may be explained by an increase in bulk and/or surface recombination, the increase in J_{sc} is more difficult to explain without invoking a decrease in apparent bandgap triggered by phase segregation. While not discussed in their report, phase segregation hence seems to appear in their case as well. Furthermore, this speculation would indicate that reverse bias-induced phase segregation is not recoverable after 3 h of MPPT, in agreement with the inability of our cells to recover from phase segregation (as discussed in the previous paragraph).

The elemental distribution observed after current-induced phase segregation, i.e. the presence of an I-rich region close to the NiO contact and a Br-rich one close the LiF/C_60 side, is likely to result from a complex interplay between lattice strain induced by carrier injection[22,23], mobility of holes and electrons in the absorber[21] and the quality of each interfaces[25]. Indeed, existing models rationalizing light-induced phase segregation models fail to fully explain our observations[18,21]. These suggest that the lower bandgap region, i.e. the I-rich one, should form close to where holes are injected in the absorber, here at the perovskite/LiF/C_{60} interface. This effect should be a consequence of the lower energy of holes in the lower bandgap part as the difference in bandgap between Br-rich and I-rich regions mainly stems from the difference in valence bands[26,27]. However, these models do not account for a key parameter that may explain the elemental distribution observed ehere after phase segregation: the difference in quality between the perovskite interfaces. Indeed, as recently reported by Belisle et al.[25], defective surfaces may accelerate phase segregation as a consequence of an increased accumulation of interfacial charges and resulting bend bending. Here, the interface between the NiO and the perovskite may contain more recombination centers than the LiF/C_{60} side, which may influence bromine and iodine differently and hence inducing the observed trend.

Figure 5 presents a summary of the degradation mechanisms observed in this work, i.e. shunt formation at the position of the metal electrode, S-shape due to iodide migration in the C_{60} and phase segregation, as a function of the reverse voltage range they occur.

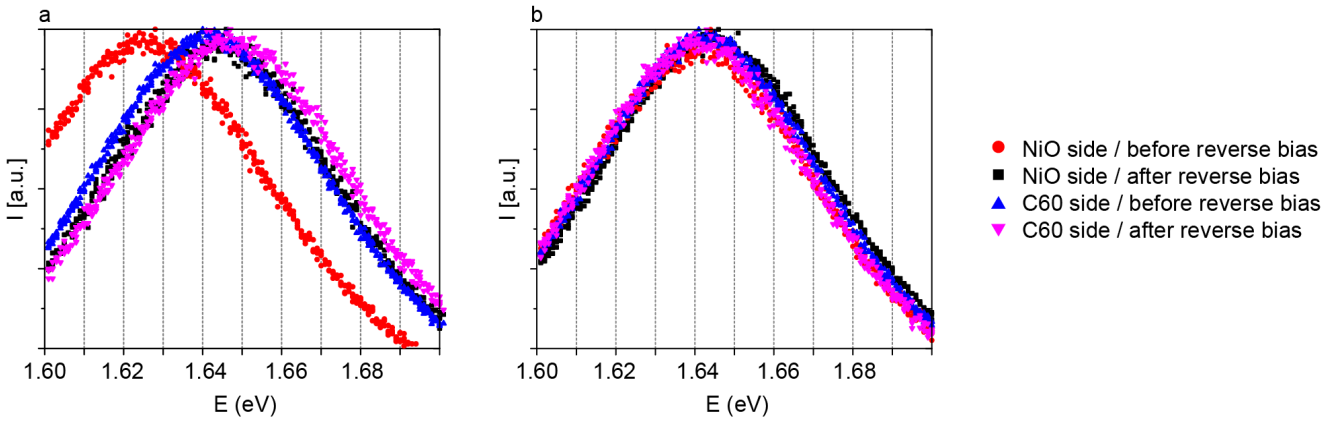

FIG. 4. Normalized photoluminescence spectra measured from the NiO and C_{60} sides before and after reverse biasing at (a) −3 V and (b) −0.5 V for 15 min. In (a), a red-shift is measured on the NiO side, while a slight blue-shift is measured on the C_{60} side, inline with the elemental map of Figure 2b. No phase segregation is observed in (b) as the applied voltage is lower in absolute value than the breakdown voltage and hence no current is flowing through the device.

III. IMPLICATIONS

Here, we discuss the criteria that must be achieved to pass the IEC partial shading test mentioned in the introduction. However, it should be emphasized that this test was not designed for perovskite solar cells and their unique degradation pathways and that it does not provide any pass/fail criteria on the power loss[2], complicating any critical assessment of the ability of this technology to pass this test. As en example of this complexity, Bowring et al.[7] observed that each cycle of reverse bias degradation-recovery at MPP yields a slower recovery rate. Such effect will not be discussed in this paragraph and the analysis will focus on irreversible effects induced by the formation of shunts and by current-induced phase segregation and changes in microstructure.

It should be first mentioned that V_{bd} has a high influence on the reverse bias stability of perovskite solar cells as it determines the maximum reverse voltage that can be applied before a reverse current starts to flow through the device. In the absence of bypass diodes, lowering V_{bd} may alleviate irreversible changes by reducing the power dissipated ($I_{mpp} \times V_{bd}$) by the shaded cell. Alternatively, a high V_{bd} becomes beneficial with bypass diodes. The number of cells per bypass diode N_{cells} to maintain a reverse voltage of V_{rev} on the shaded cell can be calculated as follows (assuming all the other cells of the string are operating normally):

$$V_{reverse} = (N_{cells} - 1)V_{mpp} + V_{bp} \quad (1)$$

where V_{bp} is the turn-on voltage of the bypass diode. Excluding the metal-induced shunt formation mechanism and assuming a V_{mpp} of 1 V and a V_{bp} of 0.3 V, two cells per bypass diode should enable to protect the device by keeping V_{rev} below (in absolute value) V_{bd} to avoid any phase segregation/microstructural changes. The number of semi-transparent cell per bypass diode decreases to 1 when taking into account the formation of shunts at the metal electrodes. The V_{rev} of $\sim$ 0.3 V that will apply on the cell in these conditions should not trigger the formation of shunts in a semi-transparent design. On the other hand, opaque cell will become shunted even with one bypass diode protecting each cell. Overall, there is an urgent need to prevent the formation of shunts before any commercialization can be envisaged.

IV. CONCLUSION

Perovskite solar cells are shown to degrade as a result of at least three different mechanisms when a reverse voltage is applied. Two of these mechanisms are irreversible for the cell design studied in this work. One involves a voltage-driven metal shunting mechanism and the other one a phase segregation accompanied by microstructure changes when a significant current flows through the cell. The third mechanism, which appears as an S-shape, seems to stem from the migration of iodide into the C_{60} from the PK into the C_{60}. This last mechanism is reversible to some extent when subjecting the cell to maximum power point tracking for at least 1 hour. The implication of these observations on the number of bypass diodes and the engineering of the breakdown of the cell to minimze damage are then discussed

V. ACKNOWLEDGEMENTS

Financial supports from the Swiss Federal Office of Energy (SI/501804-01 INTENT), the Swiss National Science Foundation (176552 Bridge Power, CRSII5_171000 Sinergia Episode), the Marie Sklodowska-Curie Individual Fellowship from the European Unions Horizon 2020 research and innovation programme (747221 POSITS)

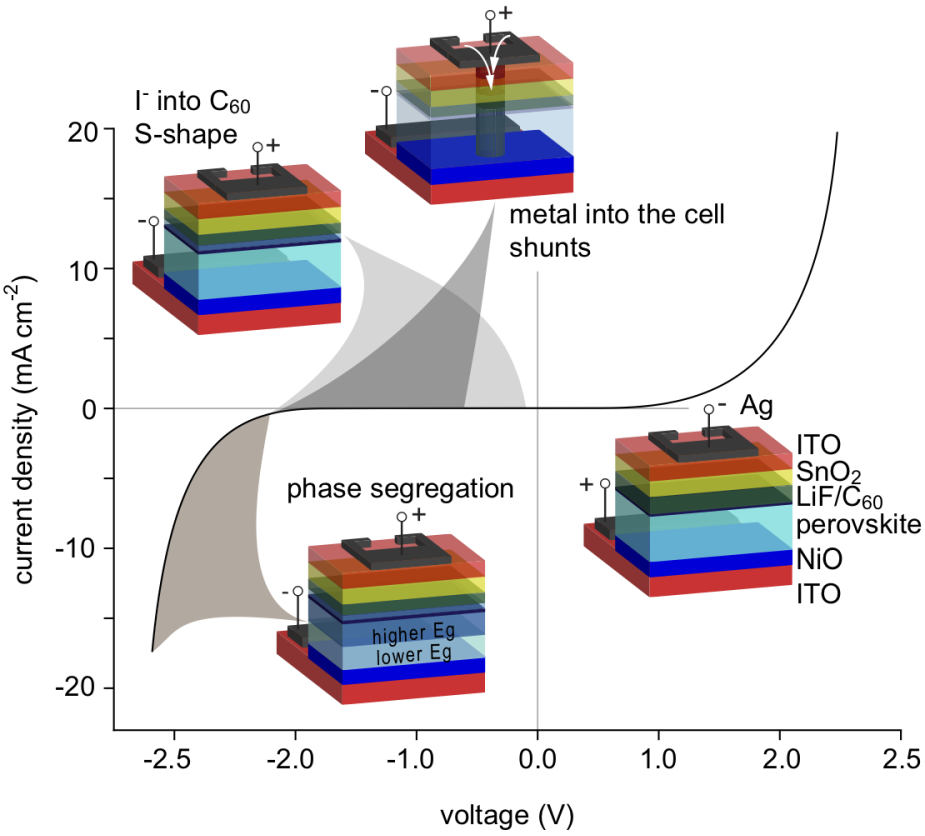

FIG. 5. Summary of the degradation mechanisms occurring during reverse biasing and the voltage range in which they occur. In this example, the breakdown voltage is ≈ -2 V, but in practice this value may range between -1 V and -4 V depending on solar cell design and processing conditions. The reverse voltages at which the mechanisms occur also depend on cell design. The three mechanisms are: 1) halogens being driven inside the C_{60} layer, which in our samples occurred for any reverse voltage applied; 2) shunt formation, which is voltage driven and becomes dominant for voltages higher than about -0.5 V; and 3) phase segregation, which only occurs for voltages higher than the breakdown voltage, when current starts to flow through the perovskite.

are gratefully acknowledged.

[1]A. Reinders, P. Verlinden, W. Van Sark, and A. Freundlich, *Photovoltaic Solar Energy: From Fundamentals to Applications* (Wiley, 2017).
[2]IEC, "International standard - thin-film terrestrial photovoltaic (pv) modules - design qualification and type approval," Tech. Rep. (International Electrotechnical Commission, 2008).
[3]S. Daliento, F. Di Napoli, P. Guerriero, and V. dAlessandro, Solar Energy **134**, 211 (2016).
[4]B. Pannebakker, A. de Waal, and W. van Sark, Progress in Photovoltaics: Research and Applications **25**, 836 (2017).
[5]Q. Zhang and Q. Li, in *Proc. IEEE Photovoltaic Specialists Conf.* (2012) p. 13441347.
[6]A. Woyte, J. Nijs, and R. Belmans, Solar Energy **74**, 217 (2003).
[7]A. Bowring, L. Bertoluzzi, B. ORegan, and M. McGehee, Advanced Energy Materials **8**, 1702365 (2018).
[8]F. Sahli, J. Werner, B. Kamino, M. Bruninger, R. Monnard, B. Paviet-Salomon, L. Barraud, L. Ding, J. Leon, D. Sacchetto, G. Cattaneo, M. Despeisse, M. Boccard, S. Nicolay, Q. Jeangros, B. Niesen, and C. Ballif, Nature Materials **17**, 820 (2018).
[9]S. Hsu, R. Whittier, and C. Mead, Solid-State Electronics **13**, 1055 (1970).
[10]o. Breitenstein, J. Bauer, K. Bothe, D. Hinken, J. Muller, W. Kwapil, M. Schubert, and W. Warta, IEEE Journal of Photovoltaics **1**, 159 (2011).
[11]M. Kntges, K. Kurtz, C. Packard, U. Jahn, K. Berger, K. Kato, T. Friesen, H. Liu, and M. Iseghem, "Performance and reliability of photovoltaic systems," Tech. Rep. (International Energy Agency, 2014).
[12]C. Buerhop and J. Bachmann, Journal of Physics: Conference Series , 012089 (2010).
[13]D. Jacobs, Y. Wu, H. Shen, C. Barugkin, F. Beck, T. White, K. Webera, and K. Catchpolea, Physical Chemistry Chemical Physics **19**, 3094 (2017).
[14]P. Calado, A. Telford, D. Bryant, X. Li, J. Nelson, B. ORegan, and P. Barnes, Nature Communications **7** (2016).
[15]Q. Jeangros, M. Duchamp, J. Werner, M. Kruth, R. Dunin-Borkowski, B. Niesen, C. Ballif, and A. Hessler-Wyser, Nano Letters **16**, 7013 (2016).
[16]Q. Zhu, D. Cox, J. Fischer, K. Kniaz, A. McGhie, and O. Zhou, Nature **355**, 712 (1992).
[17]P. Birkett, P. Hitchcock, H. Kroto, R. Taylor, and D. Walton, Nature **357**, 479 (1992).
[18]E. Hoke, D. Slotcavage, E. Dohner, A. Bowring, H. Karunadasa, and M. McGehee, Chemical Science **6**, 613 (2015).
[19]T. Duong, H. Mulmudi, Y. Wu, X. Fu, H. Shen, J. Peng, N. Wu, H. Nguyen, D. Macdonald, M. Lockrey, T. White, K. Weber, and K. Catchpole, ACS Applied Materials and Interfaces **9**, 26859 (2017).
[20]D. deQuilettes, W. Zhang, V. Burlakov, D. Graham, T. Leijtens, A. Osherov, V. Bulovi, H. Snaith, D. Ginger, and S. Stranks,

Nature Communications **7** (2016).
[21]S. Draguta, O. Sharia, S. Yoon, M. Brennan, Y. Morozov, J. Manser, P. Kamat, W. Schneider, and M. Kuno, Nature Communications **8** (2017).
[22]C. Bischak, C. Hetherington, H. Wu, S. Aloni, D. Ogletree, D. Limmer, and N. Ginsberg, Nano Letters **17**, 1028 (2017).
[23]A. Barker, A. Sadhanala, F. Deschler, M. Gandini, S. Senanayak, P. Pearce, E. Mosconi, A. Pearson, Y. Wu, A. Kandada, T. Leijtens, F. De Angelis, S. Dutton, A. Petrozza, and R. Friend, ACS Energy Letters **2**, 1416 (2017).
[24]I. Braly, R. Stoddard, A. Rajagopal, A. Uhl, J. Katahara, A. Jen, and H. Hillhouse, ACS Energy Letters **2**, 1841 (2017).
[25]R. Belisle, K. Bush, L. Bertoluzzi, A. Gold-Parker, M. Toney, and M. McGehee, ACS Energy Letters **3**, 2694 (2018).
[26]W. Yin, T. Shi, and Y. Yan, Applied Physics Letters **104**, 063903 (2014).
[27]S. Bretschneider, J. Weickert, J. Dorman, and L. Schmidt-Mendea, APL Materials **2**, 040701 (2014).